Article

Not peer-reviewed version

Unraveling Verapamil's Multidimensional Role in Diabetes Therapy: From β-Cell Regeneration to Cholecystokinin Induction

Hossein Arefanian *, Ashraf Al Madhoun, Fatema Al-Rashed, Fawaz Alzaid, Fatemah Bahman, Rasheeba Nizam, Mohammed Alhusayan, Sumi Elsa John, Sindhu Jacob, Michayla R Williams, Nermeen Abu Khalaf, Steve Shenouda, Shibu Joseph, Halemah AlSaeed, Shihab Kochumon, Anwar Mohammad, Lubaina Koti, Sardar Sindhu, Mohamed Abu-Farha, Jehad Abubaker, Thangavel Alphonse Thanaraj, Rasheed Ahmad, Fahd Al-Mulla *

Posted Date: 27 March 2024

doi: 10.20944/preprints202403.1681.v1

Keywords: β-cells; Verapamil; Calcium channel blocker; Zebrafish; MIN6 cells; Diabetes Mellitus

Article

Unraveling Verapamil's Multidimensional Role in Diabetes Therapy: From β-Cell Regeneration to Cholecystokinin Induction

Hossein Arefanian [1], Ashraf Al Madhoun [2,3,#], Fatema Al-Rashed [1,#], Fawaz Alzaid [4,5,#], Fatemah Bahman [1], Rasheeba Nizam [2], Mohammed Alhusayan [4], Sumi John [2], Sindhu Jacob [2], Michayla Williams [4], Nermeen Abukhalaf [3], Steve Shenouda [1], Shibu Kurian [6], Halemah AlSaeed [1], Shihab Kochumon [1], Anwar Mohammad [6], Lubaina Koti [2], Sardar Sindhu [1,3], Mohamed Abu-Farha [7,8], Jehad Abubaker [6], Thangavel Alphonse Thanaraj [2], Rasheed Ahmad [1] and Fahd Al-Mulla [2,*]

[1] Department of Immunology & Microbiology Department, Dasman Diabetes Institute, Dasman, 15462, Kuwait
[2] Department of Genetics and Bioinformatics, Dasman Diabetes Institute, Dasman, 15462, Kuwait
[3] Animal and Imaging Core Facility, Dasman Diabetes Institute, Dasman, 15462, Kuwait
[4] Department of Bioenergetics & Neurometabolism, Dasman Diabetes Institute, Dasman, 15462, Kuwait
[5] Institut Necker Enfants Malades (INEM), French Institute of Health and Medical Research (INSERM), Immunity & Metabolism of Diabetes (IMMEDIAB), Université de Paris Cité, Paris, France
[6] Special Services Facilities, Dasman Diabetes Institute, Dasman, 15462, Kuwait
[7] Department of Biochemistry and Molecular Biology, Dasman Diabetes Institute, Dasman, 15462, Kuwait
[8] Department of Translational Research, Dasman Diabetes Institute, Dasman, 15462, Kuwait
* Correspondence: fahd.almulla@dasmaninstitute.org; Tel.: +965 2224 2999 (ext. 2211); Fax: +965 2249 2436
# Co-authors contributed equally

Abstract: This study unveils ver.apamil's compelling cytoprotective and proliferative effects on pancreatic β-cells amidst diabetic stressors, spotlighting its unforeseen role in augmenting cholecystokinin (CCK) expression. Through rigorous investigations employing MIN6 β-cells and zebrafish models under type 1 and type 2 diabetic conditions, we demonstrate verapamil's capacity to significantly boost β-cell proliferation, enhance glucose-stimulated insulin secretion, and fortify cellular resilience. A pivotal revelation of our research is verapamil's induction of CCK, a peptide hormone known for its role in nutrient digestion and insulin secretion, which signifies a novel pathway through which verapamil exerts its therapeutic effects. Furthermore, our mechanistic insights reveal that verapamil orchestrates a broad spectrum of gene and protein expressions pivotal for β-cell survival and adaptation to immune-metabolic challenges. In vivo validation in a zebrafish larvae model confirms verapamil's efficacy in fostering β-cell recovery post-metronidazole infliction. Collectively, our findings advocate for verapamil's reevaluation as a multifaceted agent in diabetes therapy, highlighting its novel function in CCK upregulation alongside enhancing β-cell proliferation, glucose sensing, and oxidative respiration. This research enriches the therapeutic landscape, proposing verapamil not only as a cytoprotector but also as a promoter of β-cell regeneration, thereby offering fresh avenues for diabetes management strategies aimed at preserving and augmenting β-cell functionality.

Keywords: β-cells; Verapamil; Calcium channel blocker; Zebrafish; MIN6 cells; Diabetes Mellitus

1. Introduction

Consistently escalating morbidity and complications associated with diabetes have become a matter of growing concern. As of 2021, globally, 537 million (1 in 10) adults were living with diabetes, and these staggering figures are predicted to even rise up to 783 million by the 2045 [1]. Although in

 doi:10.20944/preprints202403.1681.v1

the past century, the discovery of insulin has improved the therapeutic options for patients with diabetes, certain limiting factors such as insufficient efficacy, cost, weight gain, and life-threatening hypoglycemic episodes remain the prohibitive challenges that are commonly associated with use of insulin in humans [2,3].

Type 2 diabetes mellitus (T2DM) is a chronic metabolic disorder, accounting for 90–95% of all diabetic cases. Its pathophysiology involves a combined effect of long-term insulin resistance and β-cell impairment and consequently the reduced insulin secretion and hyperglycemia, leading ultimately to pancreatic β-cell dysfunction [4]. Type 1 diabetes (T1D) is an autoimmune and inflammatory disease which is characterized by a loss of pancreatic β-cells. Its treatment is basically dependent on the exogenous insulin to maintain normoglycemia which requires continuous infusion or multiple daily injections, with no oral medications available. Moreover, treatment with exogenous insulin does not reverse the loss of β-cell mass and function [5]. Although the therapeutic approaches aimed at improving insulin delivery and glucose uptake are necessary for the treatment of diabetes, they are not designed to target the disease at its root cause i.e., β-cell dysfunction or loss.

Verapamil is a calcium channel blocker (CCB) which was approved by the Food and Drug Administration (FDA) in the late 1990s for the treatment of hypertension, angina, and arrhythmia [6]. Notably, it was found to lower the risk of developing new-onset diabetes [7–9], as compared to other CCBs; and was also found to lower fasting glucose levels in patients with diabetes [3,10–14]. Verapamil is known to act by inhibiting the L-type calcium channels and reducing the cellular calcium influx, thereby inhibiting the transcription of thioredoxin-interacting protein (TXNIP) [14–16] which would otherwise accumulate and increase oxidative stress related toxicity in the pancreas [11,17,18]. While, the intracellular calcium is required to trigger insulin exocytosis, chronic increase in the calcium levels may result in β-cell impairment [19]. This preventative mechanism of verapamil is highly attributed to TXNIP downregulation which leads to a decrease in β-cell apoptosis [14,15,19].

Verapamil ameliorated β-cell survival and activity, enhanced insulin levels, improved glucose sensitivity and homeostasis, and reduced hypoglycemic episodes in both mouse model and T1D patients [3,11,13–15]. Oral verapamil administered to patients with T1D lowered dependency on exogenous insulin and improved endogenous β-cell function, measured using the C-peptide area under the curve (AUC), as compared to placebo. Additionally, it decreased the frequency of hypoglycemic events [3,11,13–15]. Similarly, in mice, oral verapamil lowered TXNIP expression, increased endogenous insulin levels, and reduced β-cell apoptosis, rescuing the mice from streptozotocin (STZ)-induced diabetes [15,20]. In human clinical trials, verapamil showed a reduced risk of new-onset diabetes, as compared to atenolol use [8,9].

These interesting studies led us to further investigate the mechanisms of the beneficial effects of verapamil on MIN6 mouse pancreatic β-cells and transgenic zebrafish models, specifically focusing on β-cells viability and function, following challenge with immune-metabolic stressors mimicking the T1D/T2D insults.

2. Materials and Methods

Cell Culture and Treatments

MIN6 cells, a mouse β-cell line, were generously gifted by Dr. Jun-ichi Miyazaki, Kumamoto University Medical School, Japan [21]. The cells were cultured and maintained in Dulbecco's modified Eagle's medium (DMEM) which contained 25.2 mM glucose, supplemented with 15% heat-inactivated fetal bovine serum (FBS), 2 mM l-glutamine, 1 mM sodium pyruvate, 10 mM HEPES, 50 μg/mL penicillin, 100 μg/mL streptomycin, and 70 mM β-mercaptoethanol at 37°C, with 5% CO_2 (all reagents were purchased from Invitrogen, Waltham, MA, USA). The cells were re-fed every 2 to 3 days [21]. For experimental assays, cells were maintained in the supplemented DMEM containing 5.6 mM glucose. All analyses using MIN6 cells were performed at a passage of <25.

A stock solution of verapamil hydrochloride (152-11-4, Calbiochem, Burlington, MA, USA) was freshly prepared in phosphate-buffered saline (PBS). The cells were treated with verapamil at different concentrations, depending on each experimental setting.

 doi:10.20944/preprints202403.1681.v1

Cell Survival

Cells were seeded at a concentration of 5×10^4 cells/well in a 96-well plate (Costar, High Wycombe, UK). Based on the experimental set-up, cells were treated with verapamil and/or different stressors (Details included in Supplementary Methods), and cell survival was determined using an MTT (3-[4,5-dimethylthiazol-2-yl]-2,5 diphenyl tetrazolium bromide) assay (Trevigen, Minneapolis, MN, USA), following the manufacturer's instructions. Plates were read using Synergy H4 Hybrid Microplate Reader (BioTek, Winooski, VT, USA), and the data were analyzed using Gen5 software.

Cell Proliferation

MIN6 β-cell proliferation was determined by monitoring growth, consecutively for 24h. To perform proliferation assays, cells were seeded at concentration of 5×10^4 cells/well in 24-well plates (Costar, High Wycombe, UK) and incubated overnight at 37°C in 5% CO_2. Later, verapamil was added (50 μM), every 24h for 7 days, followed by trypsinization, harvesting, and cell counting using trypan blue dye exclusion assay.

Immunohistochemical Detection of Ki67

To test the effect of verapamil on MIN6 β-cell proliferation, immunohistochemical (IHC) analysis of Ki67 was performed, as described previously [22]. Briefly, cells were seeded on coverslips in media supplemented with 2% bovine serum albumin (BSA) free fatty acid (FFA) (Cat# 820024, Sigma, USA) for 24h. Then, cells were either treated with verapamil (50 μM) for another 24h or left untreated to serve as control. Cells were stained using rabbit anti-mouse Ki67 primary antibody and goat anti-rabbit secondary antibody; actin filaments and nuclei were counterstained using Phalloidin-iFluor 594 reagent and mounting medium with DAPI (Details included in Supplementary Methods) and confocal images were obtained using inverted Zeiss LSM710 spectral confocal microscope (Carl Zeiss, Gottingen, Germany). All samples were analyzed using the same parameters and the resulting color markup for analysis of each sample was confirmed. Correlated total cell fluorescence (CTCF) was calculated from 10 different fields of each number (n) via ImageJ, using the following equation:

CTCF = Integrated Density - (Area of selected cell × Mean fluorescence of background readings) [23].

Western Blotting

MIN6 cells were seeded in 6-well plates (Corning, Somerville, MA, USA), and incubated in media supplemented with 2% BSA free-FFA for 24h. Then, cells were either treated with verapamil (50 μM) and incubated for another 24h or left untreated (control). Later, total protein was extracted, and Western blotting was performed as previously described [24,25] (Details included in Supplementary Methods).

Cell Cycle Analysis

Cell cycle analysis was carried out using flow cytometry, based on propidium iodide (PI) staining of the DNA, as described before [26]. Briefly, MIN6 cells were seeded in 12-well plates (Costar, High Wycombe, UK) in media supplemented with FFA-free 2% BSA for 24h. Then, cells were treated with verapamil (50 μM) for 1, 2, 3, or 4h, or left untreated (control). Following trypsinization, re-suspended cells were fixed with ice-cold 70% ethanol, harvested by centrifugation (800 ×g for 5 min), treated at room temperature (RT) with RNase (100 μg/mL) for 30 min, followed by incubation with PI (40 μg/mL) for another 30 min. DNA content and cell cycle were analyzed using BD FACSCant Flow Cytometer (BD Bioscience, San Jose, Ca, USA). Cells were gated and analyzed for doublet exclusion. A single cell population was acquired for analysis at 490 nm Ex and 630 nm Em wavelengths. Data were analyzed using BD FACSDivaTM Software 8 (BD Biosciences, USA).

 doi:10.20944/preprints202403.1681.v1

Protection Assays

For protection assays, verapamil was used at concentrations of 1, 5, 10, and 50 μM. The protection assays were conducted for verapamil treatment in pretreatment, cotreatment, and pretreatment followed by cotreatment conditions, and challenged the cells with STZ and T1D-/T2D-cytomixes, as indicated elsewhere [27,28]. (Details included in Supplementary Methods).

Glucose-Stimulated Insulin Secretion (GSIS) Assay

A GSIS assay was performed using static incubation method, as described before [29] (Details included in Supplementary Methods). Briefly, 1×10^5 cells/well were seeded in 24-well plates (Corning, Somerville, MA, USA) and incubated for 24h. Later, MIN6 cells were treated with verapamil (50 μM) for another 24h. Then, the cells were incubated with Krebs–Ringer HEPES buffer supplemented with different concentrations of glucose at 37°C. GSIS assay was terminated, the conditioned media were collected, and levels of secreted insulin were detected using ultrasensitive mouse insulin ELISA kit (Mercordia, Sylveniusgatan, Uppsala, Sweden). Total insulin content in cells were measured by adding cold acidified ethanol to each well and keeping it overnight at -80°C. After three freeze/thaw cycles, cells were scraped off and supernatants were collected by centrifugation, neutralized with 1M Tris pH 7.5 and insulin levels were measured using ELISA. The levels of total insulin content and secreted insulin were normalized by the level of total protein measured by Bradford assay against a standard curve.

Metabolic Flux Analysis (Seahorse Assay)

Oxygen consumption rate (OCR) was analyzed by Mitochondrial Stress Test using the manufacturer's protocol (Seahorse XFe96, Agilent Technologies, Santa Clara, CA, USA). Briefly, MIN6 cells were seeded in Agilent Seahorse XF96 Cell Culture Microplate (Cat#: 101085-004) at a concentration of 4×10^4 cells/well and incubated for 24h and later, cells were either treated with STZ (3 mM) and/or verapamil (50 μM) or were left untreated (control). At the end point of each condition, an OCR assay was performed using compounds in assay media (supplemented with 5.6 mM glucose) at the following concentrations: Oligomycin (1 μM), FCCP (2 μM), and Rot/AA (0.5 μM) (Cat# 103015-100; Agilent Technologies Seahorse XF Cell Mito Stress Test Kit, Santa Clara, CA, USA). The levels of basal and maximal respirations were calculated, and OCR was normalized by the number of cells [30].

Whole-Transcriptome Analysis

Whole-transcriptome analysis was conducted as described [25] (Details included in Supplementary Methods). Briefly, total RNA was isolated from verapamil-treated (50 μM; 24h) and untreated control MIN6 cells using RNeasy kit (Qiagen, Hilden, Germany), following standard protocol. For whole-transcriptome sequencing, RNA (40 ng) was used to prepare the transcriptome libraries, using Truseq stranded mRNA kit (Illumina Inc., San Diego, CA, USA) and following the manufacturer's protocol. The libraries were validated and quantified using bioanalyzer (Agilent Technologies, Santa Clara, CA, USA) and qubit fluorometer (Thermofisher Scientific, Santa Clara, CA, USA), respectively. Paired-end sequencing was carried out using Novaseq 6000 system (Illumina Inc. San Diego, CA, USA) and the BCL files were converted to Fastq using bcl2fastq v.2.20 tool. Quality control of Fastq files was performed using FastQC (v0.11.9). Trimmomatic (v0.39) was used for adaptor and quality trimming, and for removing extremely short reads and HISAT2 (v2.1.0) for data alignment. To enumerate the number of reads associated with the genes, htseq-count tool was used in HTSeq (v 0.9.1). Differential gene expression analysis was performed using Bioconductor package edgeR, using the default setting.

Proteome Sample Preparation

Proteome sample preparation was conducted based on the standard protocol [31] (Details included in Supplementary Methods). Briefly, frozen pellets of MIN6 cells treated with verapamil (50

 doi:10.20944/preprints202403.1681.v1

μM; 24h) and untreated cells (control) were lysed, reduced using reduction buffer at 37°C, and then digested by incubating with trypsin at 37°C overnight. Next, the samples were acidified, cleaned by using C-18 MACROSpin plates, and the digested peptides were eluted in 340 μl/well of C18 elution solution (0.1% v/v) TFA in 50% acetonitrile. Samples were dried, reconstituted (1 μg/μl) and analyzed using Q-Exactive liquid chromatography-electrospray ionization-tandem mass spectrometry (LC-ESI-MS/MS) coupled with an EASY-nLC™ 1200 nano-LC System, through an EASY-Spray Ion Source (Thermo Fisher Scientific, Waltham, MA, USA). Peptides were eluted, separated using a 170-minute run, and the eluent was ionized using Easy Spray nano ESI source operating in positive ion mode. Label-free quantitation was performed using Thermo Scientific Proteome Discoverer 2.4 software and SEQUEST® HT search engine. The data were searched against a Mus musculus fastafile with a 1% false discovery rate (FDR) using Percolator. Further processing was performed using new Rt-Aligner and created Feature Mapper nodes for the untargeted label-free quantification workflow. FDRs for proteins, peptides, and peptide spectral matches were kept at 1%. All results were filtered by a q-value of <0.01 (equals an FDR of 1% on peptide level and a filter of minimum 2 unique peptides) Each experiment was performed in technical triplicates.

Bioinformatics Analyses

RNA-Seq downstream analysis was performed using in-house R scripts. The volcano plot and heatmap were generated using R packages: ggplot2 and heatmap, respectively. Functional classification and enrichment analysis were based on GO annotation and the Kyoto Encyclopedia of Genes and Genomes (KEGG) database [25]. To detect the pathways differentially perturbed in verapamil-treated cells as compared to untreated cells, a computational method was used to integrate differential gene expression into predefined pathways as previously described [32]. Briefly, P = (G, I) was graphed, where "P" is pathway, "G" is their gene sets, and "I "depicts the interactions between these genes. The fold change (treatment vs. control) data were entered and the pathways perturbed by verapamil treatment were identified. Liptak-Stouffer z-score was calculated as the perturbation of each subgraph and the most perturbed sub-pathway was computed using the algorithm as described elsewhere [32]. Bonferroni corrections were applied to compute p-values of the most perturbed pathways for more stringent proteomic and transcriptomic results.

In vivo Study Using Transgenic Zebrafish Embryos Model

Zebrafish (*Danio rerio*) were reared at 28°C under a 12-h light/dark cycle at the Dasman Diabetes Institute's Animal Facility. The fish were bred as per the guidelines approved by the Animal Care Ethical Committee (RA-2019-005), in accordance with the National Institutes of Health (NIH) guide for the care and use of laboratory animals (NIH Publications No. 8023, revised 1978) and in compliance with the ARRIVE guidelines as well as the standard laboratory procedures for zebrafish [33]. Ins:NfsB-mCherry transgenic zebrafish was a generous gift from Dr. Michael J. Parsons, University of California, Irvine, USA. In this ins:NfsB-mCherry transgenic model, the bacterial gene encoding nitro-reductase (NTR) enzyme (which converts a prodrug such as metronidazole (MTZ) to cytotoxins) was fused to mCherry fluorescent reporter, under the control of insulin proximal promoter [34]. MTZ (M3761, Sigma, St. Louis, Mo, USA) was dissolved in E3 media as described [35] and verapamil was dissolved in deionized water. Embryos were reared in E3 media at 28°C in dark and to study the β-cell protective effect of verapamil, larvae were monitored 3-6 days post fertilization (dpf) β-cell regeneration by detecting mCherry fluorescence intensity. The transgenic larvae were grouped as follows: group 1, control (untreated larvae); group 2, larvae treated with 10 μM verapamil; group 3, larvae treated with 10 μM verapamil for 24h, and then exposed to fresh E3 media containing 10 mM MTZ for 48h; and group 4, embryos treated with 10 mM MTZ at 4 dpf for 48h. Full body images (75× magnification; 200 ms exposure time) were acquired using Discovery V12 Stereo microscope (Zeiss, Jena, Germany) and Alexa Flour 594 red fluorescent emission filter.

 doi:10.20944/preprints202403.1681.v1

Statistical Analysis

The data obtained were expressed as Mean ± SEM values from at least three individual experiments. The significance of group differences was calculated using unpaired Student's t-test or one-/two-way Analysis of Variance (ANOVA) test, followed by Tukey's multiple comparisons test using GraphPad Prism 9.0 (GraphPad Software, CA, USA). P-values <0.05 were considered statistically significant, and expressed as *P<0.05, **P<0.01, ***P<0.001, or ****P<0.0001.

3. Results

Verapamil Induces Proliferation of MIN6 Cells

First, we studied the effect of verapamil on MIN6 β-cell proliferation using MTT assay and the data show a significant, dose-dependent increase in cell proliferation in response to verapamil treatments (1, 5, 10, and 50 μM), as compared to control (untreated cells) (Figure 1A). The growth curve of MIN6 cells treated with verapamil (50 μM) vs. untreated control shows a significantly increased proliferation rate (Figure 1B). We also demonstrated that β-cell proliferation was increased by verapamil under serum-starved conditions. In this regard, Ki67 expression (cyan) was significantly enhanced following treatment with verapamil (50 μM), as compared to control, indicating an increase in β-cell proliferation (Figure 1C,D). In parallel, verapamil treated cells also showed increased protein expression of phosphorylated histone H3 (PHH3), a specific mitosis and proliferation marker, compared to untreated control (Figure 1E,F).

We then asked if this effect of verapamil on β-cell proliferation was time-dependent. To this end, serum starved MIN6 cells were treated with verapamil for 1, 2, 3, and 4h, followed by cell cycle analysis. Verapamil treatment significantly increased the proportion of cells undergoing mitosis, as shown by the G2/M phase expansion. Of note, this effect was time-dependent, and longer the cells were incubated with verapamil, higher numbers of cells were detected in the G2/M phase (Figure 1G). Together, these data establish that verapamil increases the MIN6 β-cell proliferation.

 doi:10.20944/preprints202403.1681.v1

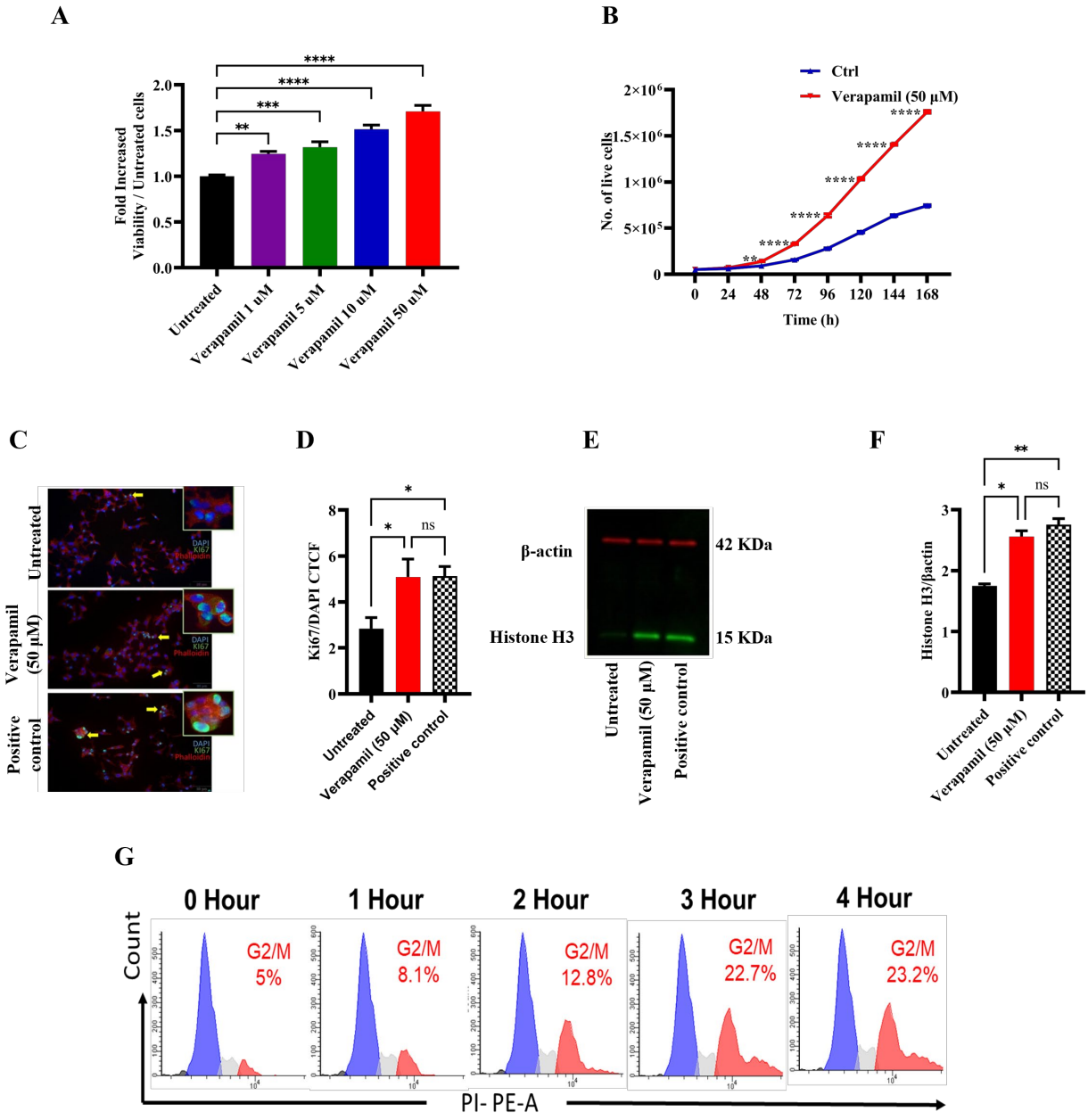

Figure 1. Proliferative effect of verapamil in MIN6 cells. (**A**) MIN6 cells were maintained in 5.6 mM glucose and were treated with different concentrations (1, 5, 10, and 50 µM) of verapamil for 24 hours. (**B**) Growth curve of MIN6 cells cultured in 5.6 mM glucose media and treated with verapamil (50 µM, Red line), in comparison with untreated cells (Blue line). (**C**,**D**) Ki67 analysis showing the influence of verapamil on cell proliferation. MIN6 cells were cultured in serum free conditions in the presence or absence of verapamil. Cells cytoskeletons were labeled with phalloidin (red) and the proliferation level was monitored with the expression of KI67 protein (green). DAPI was used to counterstain the nucleus. Scale bar = 50 µM, n= 2. The corrected total cell fluorescence (CTCF) was calculated from 10 different fields of each (n) number. (**E**,**F**) Western blot analysis of histone H3 expression corrected to β-actin with representative immunoblots, n=2. Flow cytometry analysis was conducted to investigate the influence of verapamil induction in a time-dependent manner. (**G**) Histograms of the cell cycle phases. n=4. Data are presented as mean ± SEM values and were analyzed using one-way ANOVA with Tukey's multiple comparisons test. ns = non-significant, *p≤0.05, **p≤0.01, ***p≤0.001, ****p≤0.0001 versus control.

 doi:10.20944/preprints202403.1681.v1

Verapamil Pretreatment Protects the MIN6 β-Cells from Cytotoxic Insults induced by STZ and T1D-/T2D-Cytomixes

We next asked whether verapamil was also cytoprotective, in addition to promoting the proliferation of MIN6 β-cells. To this effect, cells were either treated with verapamil or left untreated for 24h, followed by treatment with STZ (3 mM) for another 24h. As compared to cells treated with STZ alone (control), verapamil-treated cells showed significantly increased viability in a dose-dependent manner (Figure 2A). Next, MIN6 cells were co-treated (STZ plus verapamil) for 24h and, as expected, the cells exposed to verapamil (except 1 μM concentration) showed significantly increased viability, compared to cells treated with STZ only (Figure 2B). To determine if the pretreatment had a boosting effect on β-cell viability, cells pretreated with verapamil were exposed to a combined challenge with STZ plus verapamil for 24h. The cells pretreated with verapamil demonstrated a significantly higher viability, compared to cells with no verapamil pretreatment (Figure 2C). Together, these data support that verapamil has a cytoprotective effect against STZ toxicity, and the pretreatment with verapamil offers a better protection.

Given that the increased expression of IL-1β, TNF-α, INF-γ and their combined effect results in an enhanced vulnerability of pancreatic β-cells to autoimmune destruction [36], we asked whether verapamil exposure could protect the MIN6 β-cells from cytotoxic effects of these cytokines in our T1D-Cytomix model. To this end, MIN6 β-cells were pretreated with verapamil or left untreated (control) for 24h, followed by a 24h-challenge with T1D-cytomix containing IL-1β (50 ng/ml), TNF-α (50 ng/ml), and INF-γ (100 ng/ml) to mimic the T1D pancreatic cytokine microenvironment in clinical setting, and the cell viability was determined by MTT assay. We found that the cells pretreated with verapamil exhibited a significantly increased viability in a dose-dependent manner, as compared to control (Figure 2D). Similarly, the cells cotreated with verapamil plus T1D-cytomix showed significantly higher viability as compared to untreated control (Figure 2E). Next, cells were pretreated with verapamil for 24h and then challenged by verapamil/T1D-cytomix co-treatment, and no significant differences in cell viability were observed between two differentially verapamil-treated groups; however, both verapamil-treated groups had a significantly higher cell viability, as compared to control (Figure 2F).

The low-grade chronic inflammation induced by obesity is known as a main risk factor for T2D [37]. We further asked whether verapamil also had β-cell cytoprotective effect against the stressors that mimicked the T2D-associated pancreatic microenvironment. To this effect, MIN6 β-cells were treated with verapamil or left untreated (control) for 24h, and then challenged by a T2D-cytomix containing IL-1β (50 ng/ml), TNF-α (50 ng/ml), and palmitic acid (500 μM) to mimic the T2D microenvironment. After 24h, cell viability was assessed by MTT assay. As expected, the cells pretreated with verapamil showed significantly increased viability as compared to control (Figure 2G). Likewise, cells cotreated with verapamil and T2D-cytomix also showed significantly increased viability, as compared to verapamil-lacking control (Figure 2H). Moreover, no significant difference in cell viability were observed between verapamil pre-treated plus co-treated and pre-treated only groups; while both groups had a significantly higher viability, as compared to verapamil-untreated control (Figure 2I).

 doi:10.20944/preprints202403.1681.v1

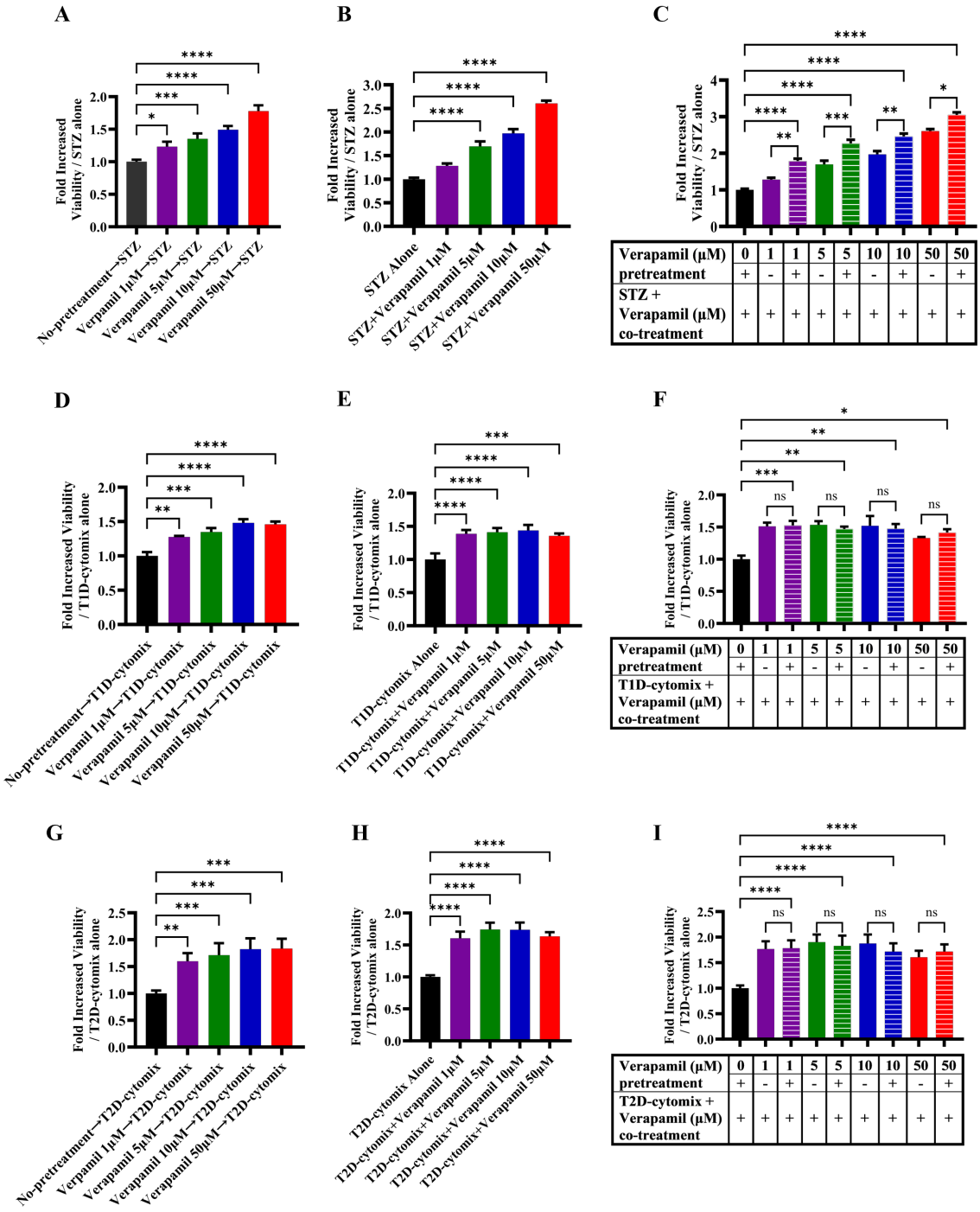

Figure 2. Protective effect of verapamil in MIN6 cells exposed to STZ, T1D-cytomix, or T2D-cytomix stressors. Bar graphs presenting MTT assay results as ratio of each treatment over viability of MIN6 cells maintained in 5.6 mM glucose. (**A–C**) Cells were stressed with streptozotocin (STZ). (**A**) Cells were pretreated with different concentrations (1, 5, 10, and 50 μM) verapamil for 24 hours, the media were changed, and cells were stressed by 3 mM of STZ for another 24 hours. (**B**) Cells were treated with a combination of STZ (3 mM) and verapamil (1, 5, 10, and 50 μM) for 24 hours. (**C**) Cells were pretreated with verapamil (1, 5, 10, and 50 μM) for 24 hours, then fresh media containing both STZ (3 mM) and verapamil (1, 5, 10, and 50 μM) were supplied to the cells for another 24 hours. (**D–F**) Cells were stressed with T1D-cytomix (IL-1β: 50 ng/ml, TNF-α: 50 ng/ml, and INF-γ: 100 ng/ml) in each setting independently. (**D**) Cells were pretreated with different concentration (1, 5, 10, and 50 μM) of verapamil for 24 hours, then media were changed, and cells were stressed with T1D-cytomix for another 24 hours. (**E**) Cells were treated with a combination of T1D-cytomix and verapamil (1, 5, 10, and 50 μM) for 24 hours. (**F**) Cells were pretreated with verapamil (1, 5, 10, and 50 μM) for 24

 doi:10.20944/preprints202403.1681.v1

hours, then fresh media containing both T1D-cytomix and verapamil (1, 5, 10, and 50 μM) were supplied to the cells for another 24 hours. (**G–I**) Bar graphs presenting MTT assay results as ratio of each treatment over viability of cells stressed by T2D-cytomix (IL-1β: 50 ng/ml, TNF-α: 50 ng/ml, and Palmitic Acid: 500 μM) in each setting independently. (**G**) Cells were pretreated with different concentration (1, 5, 10, and 50 μM) of verapamil for 24 hours, then media were changed, and cells were stressed with T2D-cytomix for another 24 hours. (**H**) Cells were treated with a combination of T2D-cytomix and different concentration (1, 5, 10, and 50 μM) of verapamil for 24 hours. (**I**) Cells were pretreated with different concentration (1, 5, 10, and 50 μM) of verapamil for 24 hours, then fresh media containing both T2D-cytomix and different concentration (1, 5, 10, and 50 μM) of verapamil were supplied to the cells for another 24 hours. Each experiment was performed at least by 5 independent repeats. Difference between the groups was statistically analyzed by two-way analysis of variance (ANOVA) and p values < 0.05 considered as a significant difference. Data are presented as Mean ± SEM, * p-value< 0.05, ** p-value <0.01, *** p-value <0.001, and **** p-value <0.0001.

Verapamil Enhances Pancreatic β-Cell Function and Glucose Sensing in MIN6 Cells

To determine whether verapamil affects insulin production and the function of MIN6 β cells, total insulin content was compared in verapamil-treated (50 μM) and untreated (control) cells. To this end, no significant difference was found between the two conditions (Figure 3A). Next, MIN6 β-cells were stimulated with different glucose concentrations to determine GSIS response to verapamil (50 μM) for 24h, compared to untreated control. The data show that GSIS was significantly enhanced ($p < 0.05$) in verapamil-treated cells exposed to 5.6, 8.4, 11.2, and 16.8 mM glucose, as compared to control (Figure 3B). Measuring insulin content in parallel, verapamil-untreated cells showed significantly higher ($p < 0.05$) insulin content after stimulation with 5.6 mM and 8.4 mM of glucose, as compared to verapamil-treated cells (Figure 3C). Based on the above findings, we further aimed to determine the glucose sensing capability and function of MIN6 β-cells by calculating the percentage of secreted insulin over total insulin content. The results show that verapamil-treated MIN6 β-cells were relatively more sensitized to glucose stimulation at designated glucose concentrations, and the percentages of secreted insulin over total insulin content differed significantly between verapamil-treated and -untreated β-cells under high glucose challenge (16.8 mM; $p < 0.01$) (Figure 3D). This data indicates that verapamil enhances β-cells glucose sensing and insulin secretion.

 doi:10.20944/preprints202403.1681.v1

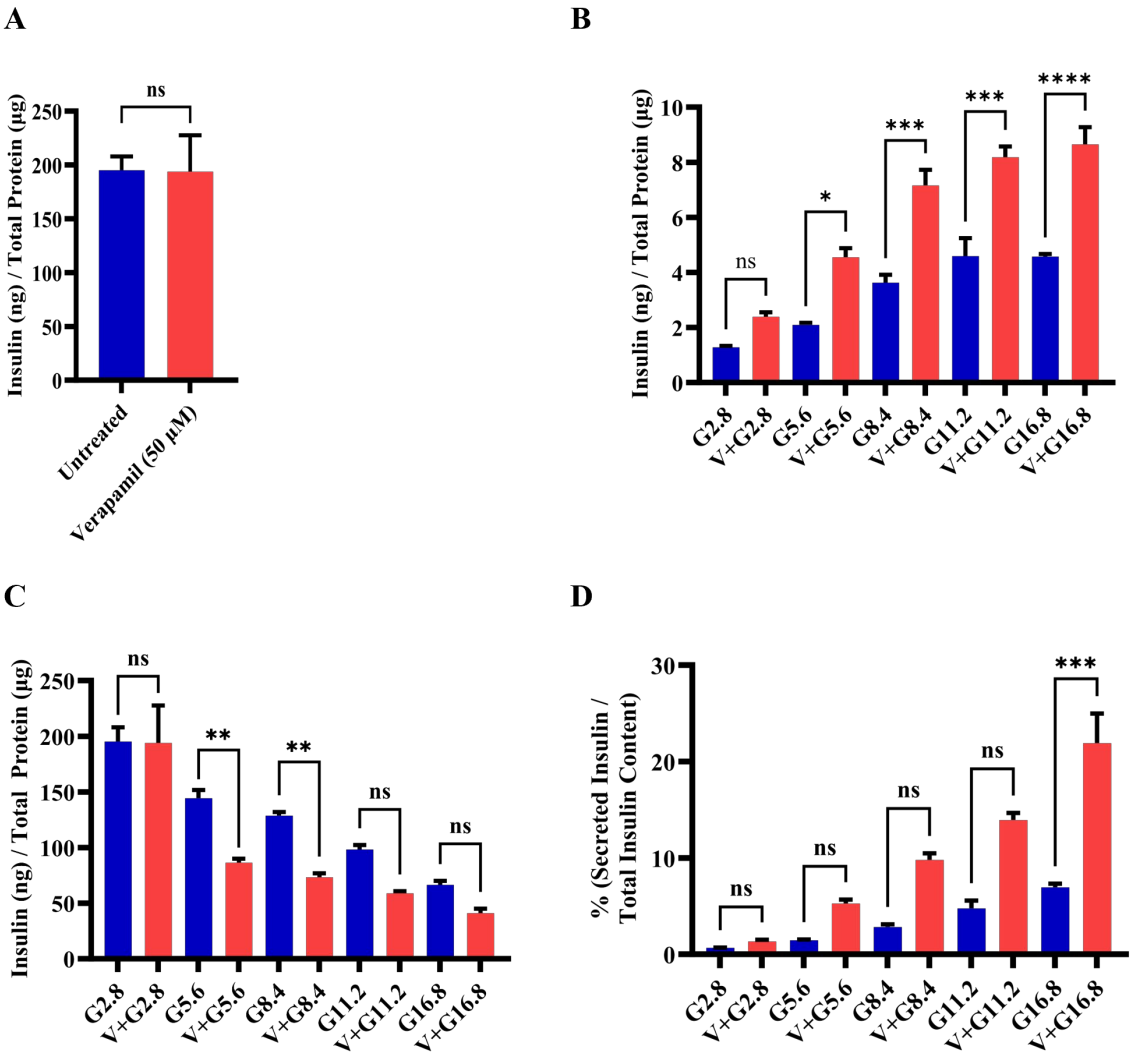

Figure 3. Functional effect of verapamil on the insulin content and glucose stimulated-insulin secretion (GSIS) rate of MIN6 cells. (**A**) Measured insulin content in MIN6 cells treated with 50 µM verapamil (Red) for 24 hours or left untreated (Blue). (**B**) Total secreted insulin by MIN6 cells and (**C**) Total insulin content in MIN6 cells, when stimulated with different concentrations of glucose and either treated with 50 µM verapamil (Red) for 24 hours or left untreated (Blue). (**D**) Percentage of secreted insulin over total insulin content of each condition. Each experiment was performed in 4 independent repeats. Difference between the groups was statistically analyzed using two-way analysis of variance (ANOVA) and p-values < 0.05 were considered statistically significant. Data are presented as Mean ± SEM; * p-value < 0.05; ** p-value < 0.01; *** p-value <0.001; and **** p-value <0.0001.

Verapamil Treatment Promotes Mitochondrial Respiration in MIN6 β-Cells

Given the critical role of mitochondrial function in insulin secretion, we next proceeded to investigate the mitochondrial respiration in MIN6 β-cells, following treatment with verapamil. To this end, MIN6 β-cells were cultured in medium containing 5.6 mM glucose and were either treated with verapamil (50 µM) for 24h or left untreated (control), and later subjected to metabolic flux analysis. In metabolic flux analysis, β-cells treated with verapamil showed significantly increased oxygen consumption (Figure 4A), including the basal respiration (Figure 4B) and maximal respiration (Figure 4C) levels, as compared to untreated control. To determine the effect of verapamil pretreatment on mitochondrial respiration in STZ-stressed MIN6 β-cells, the cells were cultured with verapamil (50 µM; 24h) and subsequently treated with STZ for another 24h, followed by metabolic

 doi:10.20944/preprints202403.1681.v1

flux analysis. We found that verapamil pretreated cells had significantly higher oxygen consumption than verapamil-untreated control challenged with STZ only (Figure 4D). Moreover, verapamil pretreatment significantly increased both the basal respiration (Figure 4E) and maximal respiration (Figure 4F). Altogether, a higher OCR at both basal and maximal levels in verapamil pretreated cells indicates that the β-cells are metabolically active, viable, and potentially functional; and that the verapamil exposure prior to STZ challenge might additionally confer a protective effect on MIN6 β-cell functionality.

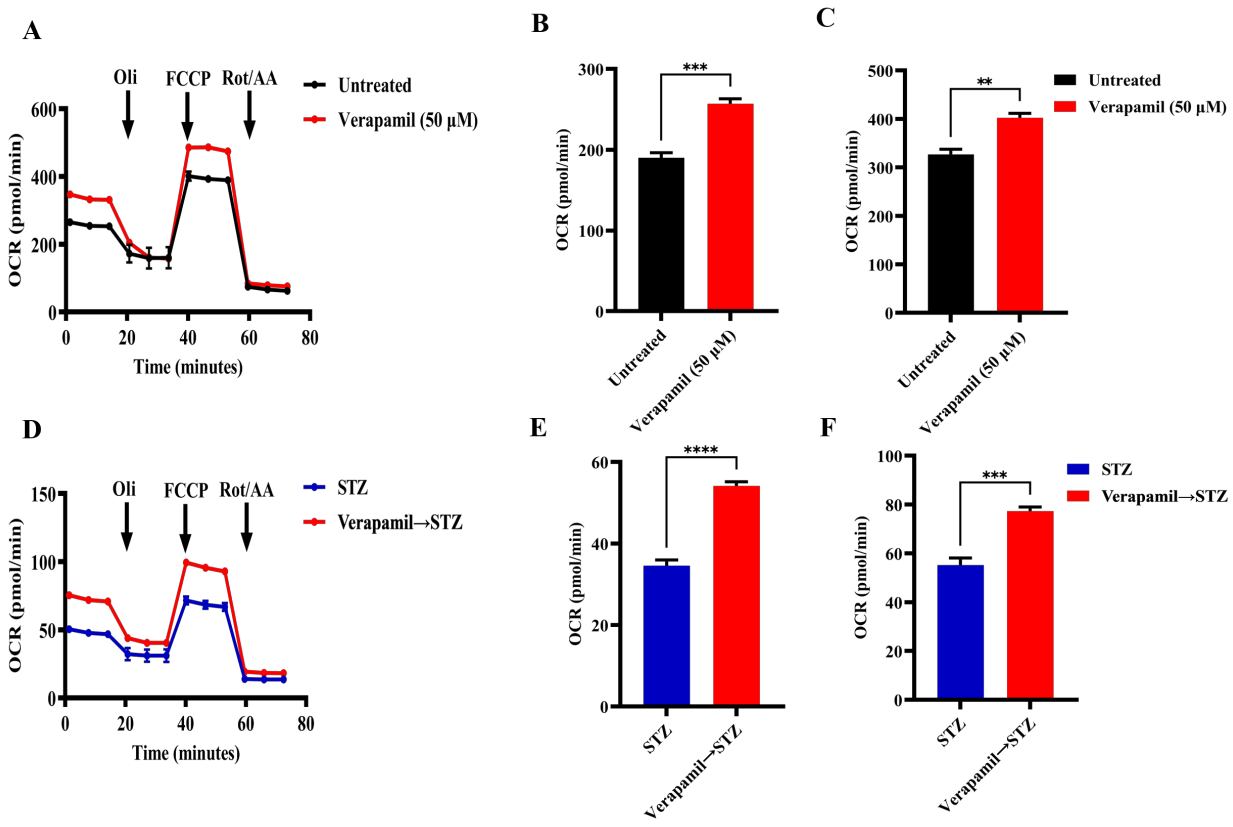

Figure 4. Verapamil pretreatment increases mitochondrial respiration in MIN6 cells treated with streptozotocin. MIN6 cells (4 × 10^4) were cultured in 5.6 mM glucose media and treated overnight with verapamil (50 µM) or were left untreated. Cells were subsequently treated with streptozotocin (STZ, 3 mM) or left untreated and subjected to metabolic flux analysis. (**A**) Metabolic flux analysis measured oxygen consumption as cells were treated with Oligomycin (1 µM), Carbonyl cyanide 4-(trifluoromethoxy)phenylhydrazone (FCCP, 2 µM), and Rotenone/Antimycin A (Rot/AA, 0.5 µM). (**B**) Basal respiration in metabolic flux analysis, point before Oli administration. (**C**) Maximal respiration in metabolic flux analysis, point before Rot/AA administration. (**D**) Metabolic flux analysis of cells pretreated with verapamil prior to STZ treatment. (**E**) Basal respiration and (**F**) maximal respiration in metabolic flux analysis of cells pretreated with verapamil. Difference between the groups was statistically analyzed using two-way analysis of variance (ANOVA) and p-values < 0.05 were considered statistically significant, n=4 per group, p-value < 0.05; ** p-value < 0.01; *** p-value <0.001; and **** p-value <0.0001.

Transcriptomic and Proteomic Profiling of Verapamil-Treated MIN6 β-Cells

To further identify the molecular mechanisms underlying the above-mentioned potential benefits of verapamil on MIN6 β-cells, the changes in gene and protein expression profiles after verapamil treatment were studied using RNA sequencing and proteomics, respectively. Comparing verapamil-treated and -untreated cells cultured in 5.6 mM glucose milieu, 2131genes and 114 protein targets were identified, of which, 32 targets were differentially expressed at both gene and protein

 doi:10.20944/preprints202403.1681.v1

levels (Figure 5A,B, Table 1). The datasets generated from the current study are available in the GEO repository (GEO accession No. GSE230803).

We used the impact analysis method [38–40] to identify the overrepresented differentially-expressed proteins in each pathway and the perturbation in that pathway, as computed by the measured expression across the pathway topology. After FDR and Bonferroni corrections, cardinal signaling pathways were represented in proteomic signatures from our samples, including those associated with the pancreatic secretion, cGMP-PKG signaling, cAMP signaling, diabetic cardiomyopathy, and calcium signaling (Figures 5C,D). The most significantly represented pathway i.e., pancreatic secretion, was further interrogated, and overall pathway perturbation was represented using KEGG resource diagrams (Figure S1A–C). An expression heatmap revealed similar patterns in up- or down-regulation between the gene and protein expression for each target, except for VDAC1 and VDAC2, indicating possible post-transcriptional regulation (Figure 5E). The most upregulated target at both the mRNA and protein levels in response to verapamil treatment was cholecystokinin (CCK), which we further confirmed using Western blot analysis (Figure 5F).

 doi:10.20944/preprints202403.1681.v1

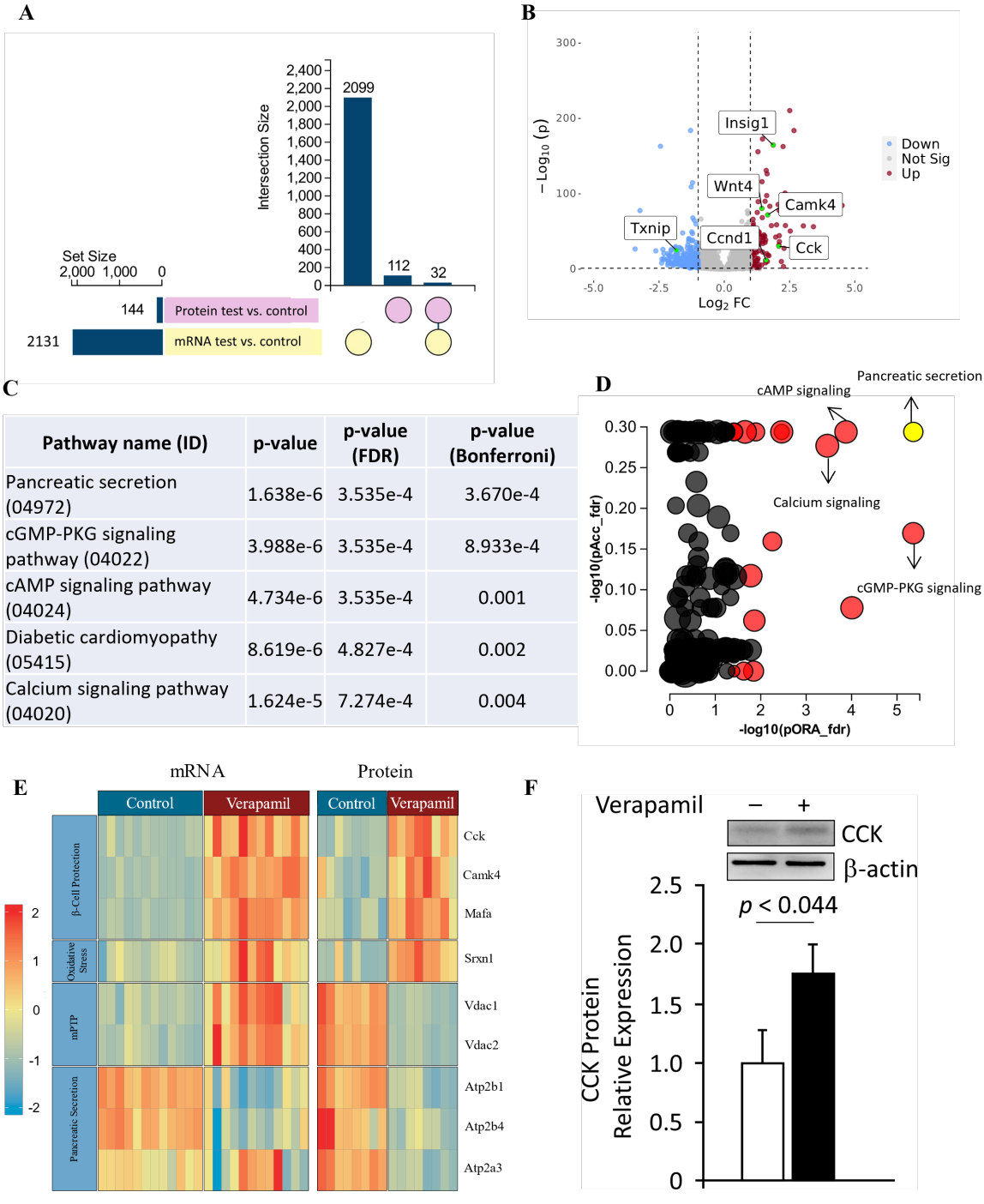

Pathway name (ID)	p-value	p-value (FDR)	p-value (Bonferroni)
Pancreatic secretion (04972)	1.638e-6	3.535e-4	3.670e-4
cGMP-PKG signaling pathway (04022)	3.988e-6	3.535e-4	8.933e-4
cAMP signaling pathway (04024)	4.734e-6	3.535e-4	0.001
Diabetic cardiomyopathy (05415)	8.619e-6	4.827e-4	0.002
Calcium signaling pathway (04020)	1.624e-5	7.274e-4	0.004

Figure 5. Transcriptomic and proteomic landscape of MIN6 cells treated with verapamil. (**A**) Out of a set size of 2131 genes (yellow) and proteins (pink), 2099 genes and 112 proteins were found to be differentially expressed. Of these, shared differential expressions of 32 genes and proteins were observed. (**B**) Volcano plot showing differentially expressed genes in MIN6 mouse beta cell line treated with verapamil (50 uM) for 24 hours ($|FC| > 2$, $p < 0.05$). (**C**,**D**) Perturbation vs. Over-representation Pathway Plot: Dots representing the top 10 impacted pathways are positioned by their p-values from two different analyses: an Impact analysis measuring total perturbation accumulation (pAcc) vs. a classical Over-representation analysis (pORA). Pathways with significant combined P-values are shown in red. The selected pancreatic secretion pathway is shown in yellow. The size of each dot denotes the total number of genes in the corresponding pathway. (**E**) Protein and mRNA levels of key genes found to be up- or down-regulated when exposed to verapamil treatment, along

 doi:10.20944/preprints202403.1681.v1

with their respective molecular functions shown in the y axis. Each cell depicts one independent experiment. The expression profiles of the respective genes are depicted by color gradient ($p < 0.05$, $|log2FC| > 1$). (**F**) Western blot analysis of CCK expression normalized to β-actin expression; a representative immunoblot is shown.

Table 1. Up-regulated and down-regulated 32 proteins and their respective genes identified by proteomics/transcriptomics analyses.

Gene name	logfc protein (mass spec)	adjpv protein (mass spec)	logfc mRNA (RNA-seq)	adjpv mRNA (RNA-seq)
Acss2	0.546956178	0.045430822	1.468439926	0.000001
Ap3m2	-1.258425153	0.004563029	-0.631083607	0.00535079
Atad1	-0.878321443	0.003214256	-0.69090951	0.001886914
Atl3	-0.775959726	0.01924926	-0.705494101	0.000782498
Atp2b1	-0.768567592	0.001599313	-0.903858193	0.00000179
Cadm1	6.64385619	0.000001	-1.111895426	0.000001
Camk4	0.618238656	0.025051947	1.667580225	0.000001
Cck	1.343692069	0.000001	2.086382128	0.000001
Fdps	1.236339539	0.000001	2.06424327	0.000001
Fn1	0.750177706	0.00019395	0.707236676	0.000001
Gabarap	0.779049553	0.000817148	0.608883531	0.000001
Gc	0.575312331	0.010226369	-0.668515132	0.000001
Gdap1	-0.744197163	0.03032308	-0.715727824	0.009402028
Hax1	6.64385619	0.000001	0.708603816	0.000001
Hectd1	1.205392513	0.000001	-0.766523599	0.004572659
Hmgcs1	1.608809243	0.000001	1.574403987	0.000001
Idi1	1.136191386	0.000001	1.063478538	0.00444946
Ins2	-0.706041021	0.003576738	-1.047050788	0.000001
Kif23	-0.899695094	0.029438363	-1.278078727	0.000001
Ldlr	1.607862903	0.000001	1.459525662	0.000001
Mafa	0.715454127	0.019937366	0.86170978	0.000001
Mid1ip1	0.82130204	0.000734422	0.902299589	0.000001
Nsg1	0.568518598	0.029438363	0.821403563	0.000001
Pam	0.600269754	0.008748346	0.772163694	0.000001
Ppfia2	-2.53951953	0.000001	-1.455788602	0.000001
Prlr	0.619178216	0.031249276	-0.938951004	0.003238752
Sdf2l1	0.606915942	0.007338519	1.333480725	0.000001
Slc25a1	-0.798366139	0.005415551	0.796013338	0.000001
Slc9a3r1	0.508935662	0.025006868	0.846755275	0.000001
Sqstm1	0.789103218	8.91352E-05	0.605062208	0.000001
Stc1	0.804053559	0.000223206	1.114392736	0.000001
Timm8b	0.670840336	0.003900441	0.676846573	0.000001

Verapamil Confers Protection from MTZ-Mediated Pancreatic β Cell Damage in Transgenic Zebraifish Model

Next, we used transgenic Ins:NfsB-mCherry zebrafish embryo model to study whether verapamil could protect from MTZ-mediated cytotoxic damage to the pancreatic β cells. The embryos were divided into following four groups: Group 1, untreated; Group 2, treated at 3 days post-fertilization (dpf) with verapamil (10 μM) for 72h; Group 3, treated at 3 dpf with verapamil (10 μM)

 doi:10.20944/preprints202403.1681.v1

for 24h, followed by drug removal and MTZ (10 mM) treatment for 48h; and Group 4, treated at 4 dpf with MTZ (10 mM) for 48h. mCherry fluorescence protein (ChFP) fluorescence intensity was detected at 4 dpf (T0) and 6 dpf (T1). We found that verapamil pretreatment embryos (Group 3) showed a significantly higher ($p = 0.015$) fluorescence intensity, as compared to verapamil-untreated embryos (Group 4) (Figures 6B,C). This indicates that verapamil induces pancreatic β-cell protective effect against MTZ cytotoxicity in zebrafish model.

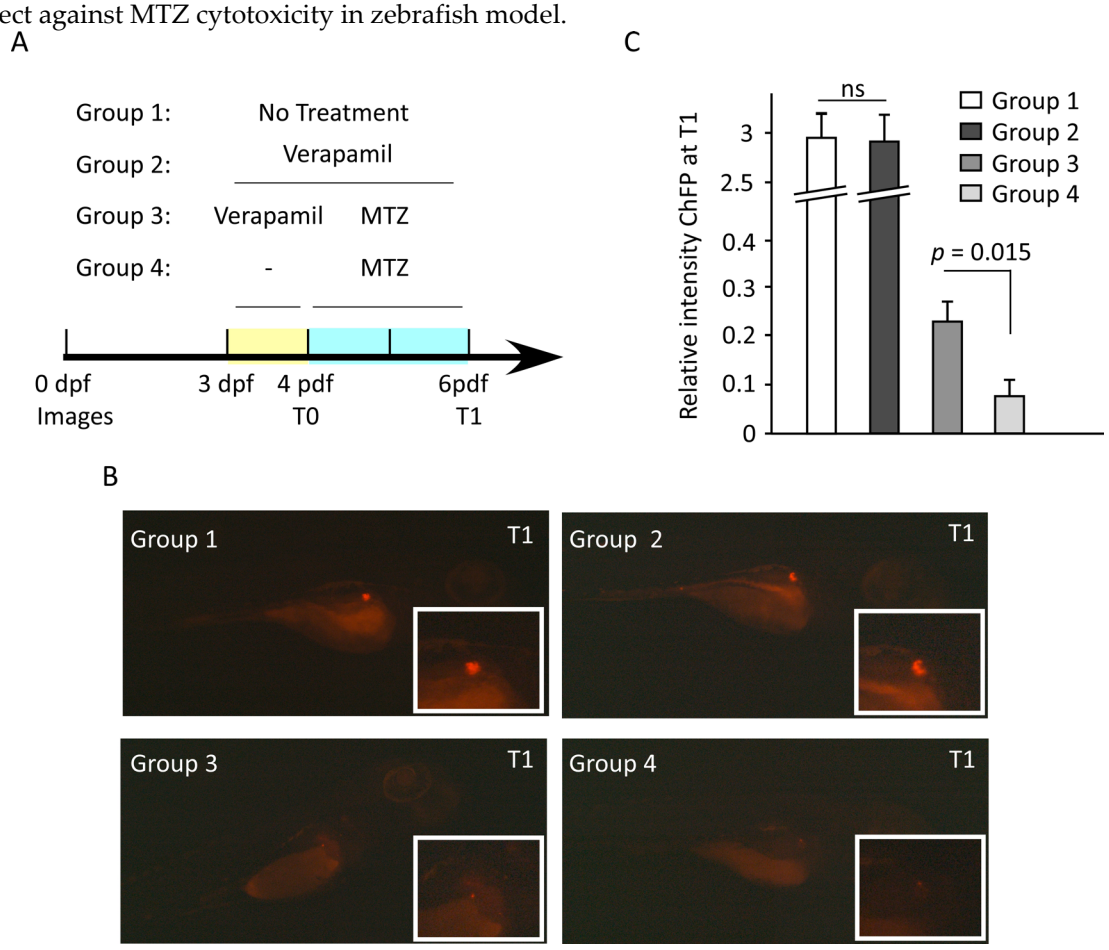

Figure 6. Verapamil pretreatment protects the pancreatic cells against MTZ-induced cytotoxic damage in zebrafish embryos. (**A**) Schematic timeline showing the experimental design and drug treatments. At 3 days post fertilization (dpf), four groups of embryos were treated as following: group 1, untreated embryos; group 2, embryos treated with 10 μM verapamil for 72 h; group 3, embryos treated with 10 μM verapamil for 24 h, followed by drug removal and administration of 10 mM MTZ for 48 h; group 4, embryos treated with 10 mM MTZ at 4 dpf for 48 h. Insulin-producing pancreatic cells co-expressing mCherry fluorescence reporter protein (ChFP) were imaged at 4 dpf (T0) and 6 dpf (T1). For each group, the differences in ChFP intensity between T0 and T1 were determined. (**B**) Representative images of pancreatic cells in each group at T1. Inserts depict the magnified ChFP area. Images were taken using Stereo discovery 1.2 ZIESS microcopy **(C)** Quantification of ChFP intensity in four groups at T1. No significant difference in fluorescence intensity was found between groups 1 and 2. However, the fluorescence intensity in group 3 which was pretreated with verapamil was significantly higher, as compared to group 3 which was not pretreated with verapamil. Experiments were done in triplicates (n = 20–30 embryos/group). Data represents the Mean ± SEM values. ns: non-significant.

4. Discussion

Insulin-producing pancreatic β-cells are the key players in glucose homeostasis and their loss is associated with the development of T1D and the progression of T2D [4,5]. Not surprisingly, residual β-cell function has been associated with reduced incidence of microvascular complications in both T1D and T2D [41,42]. Currently, promising antidiabetic therapeutic strategies aim at rescuing or

 doi:10.20944/preprints202403.1681.v1

preserving the β-cell function and insulin secretory capacity. Herein, we investigated the β-cell cytoprotective and insulinotropic effects of verapamil using T1D- and/or T2D-mimicking stressor challenges in MIN6 β-cells and transgenic zebrafish models. In our MIN6 T1D/T2D stressor models, verapamil treatment improved the β-cell viability/proliferation in a dose- and time-dependent manner, as supported by increased expression of Ki67/H3 proliferation markers and evidence of actively replicating β-cells in the G2/M phase. Moreover, in verapamil-treated β-cells, an increase in the insulin secretion was observed under high glucose culture conditions. Indeed, the normalized secreted insulin in verapamil-treated cells was significantly promoted only under the condition of high glucose (16.8 mM) stimulation, compared to the lower glucose concentrations tested in our model. It implies that β cells get hypersensitized by abnormally high glucose levels, a notion which has previously been associated with enhanced blood glucose control and reduction in exogenous insulin requirements [11,13]. Together, these observations lead to the conjecture that verapamil may rather have a more promising insulinotropic benefit under advanced hyperglycemic conditions.

Notably, while most other studies evaluated verapamil use in diabetic cohorts, we assessed its direct β-cell protective and insulinotropic effects using modified, more clinically relevant models in setting of verapamil pre-treatments or co-treatments, followed by diverse cytotoxic challenges including T1D-/T2D-cytomixes. The β-cell protective effect was further confirmed at the organismal level using MTZ-mediated β-toxicity in mCherry-reporter zebrafish embryos. We found a significantly enhanced β-cell viability in presence of verapamil in both *in vitro* and *in vivo*, establishing its preventative and β-protective benefits, in line with previous evidence that verapamil lowers the risk of new-onset T2D [3,7,8,11,13,14].

Our analyses of changes in the proteomic and transcriptomic landscapes in verapamil-treated MIN6 β-cells are of particular interest. It is noteworthy that the treatment with verapamil brought to light a wide array of proteins and genes that were differentially expressed in MIN6 β-cells. Of those, some are remarkable, owing to their involvement in fundamental pathways ultimately contributing toward maintaining glucose homeostasis and/or preserving pancreatic β-cells. In our transcriptomic analysis, we found *Ccnd1* upregulated at the mRNA level, and the role of this gene in inducing β-cell proliferation is well established [43,44]. In addition, through transcriptome analysis we also detected the lower expression of *Txnip* gene in verapamil-treated, compared to untreated cells. TXNIP, a redox regulator, was identified as an attractive therapeutic target for restoring β-cells dysfunction, owing to its increased expression in the β-cells of diabetic patients [17,20]. TXNIP overexpression is known to play a key role in β-cell apoptosis, whereas its deficiency promotes the endogenous β-cell survival [17,20,45]. Thioredoxin, a protein involved in the antioxidant defense system of β-cells, is inhibited by TXNIP, thereby promoting oxidative stress. Moreover, TXNIP is also associated with inflammasome activity, and its downregulation may have anti-inflammatory effects [46].

In response to verapamil, the most dominantly upregulated factor, at both mRNA and protein levels, was the glucose-like peptide-1 (GLP-1)-induced incretin — called cholecystokinin (CCK). To the best of our knowledge, we are the first to show that verapamil induces expression of *CCK* transcripts and proteins in MIN6 β-cells. CCK plays a role in preserving β-cell mass with increasing age and protecting them against apoptosis induced by STZ and β-toxic proinflammatory cytokines [47]. In our *in vitro* studies, verapamil induced β-cell protection against insults including STZ and T1D-/T2D-cytomixes, which could be due, in part, to upregulated CCK expression.

We also found upregulated levels of *Wnt4*, which is a ligand heterogeneously expressed in β-cells and it plays a central role in activating calcium signaling and lowering blood glucose levels, along with regulating cellular redox homeostasis [48]. Wnt4 is the most abundantly expressed protein in β-cells in high fat, high glucose, or insulin-resistant conditions; and it is suggested to play a pivotal role in β-cell proliferation or regulating and enhancing the insulin secretory response induced by the above-mentioned conditions [49]. Kurita et al. suggested that *Wnt4* might possibly be involved in glucose-induced vesicle transport of insulin in MIN6 β-cells [49]. Moreover, *Wnt4* overexpression was shown to upregulate genes controlling β-cell maturation and function and related with higher mitochondrial abundance [48].

 doi:10.20944/preprints202403.1681.v1

An increase in both mRNA and protein levels of CaMK4 upon verapamil treatment in our study is suggestive of its impact on MIN6 β-cell survival and proliferation. CaMK4, a serine/threonine kinase, has been previously shown to mediate *Irs2* expression in MIN6 cells and mouse islets stimulated by glucose, *via* the activation of cAMP response element binding protein (CREB) [50]. The present study, based on previous knowledge that *Irs2* knockout reduces β-cell mass and increases β-cell apoptosis, suggests that CaMK4 may regulate β-cell survival and proliferation, possibly *via* the IRS2-dependent stimulation of cell proliferation and apoptosis inhibition.

In this study we found higher level of basal and maximal mitochondrial respiration in verapamil-treated MIN6 β-cells which could be attributed to higher *Wnt4* expression, and that, along with reduced TXNIP gene expression could possibly explain the ability of verapamil to render protection against stressors [15]. Indeed, several studies showed that verapamil treatment reduced the pro-apoptotic TXNIP expression, thereby promoting the survival of β-cells and preventing diabetes [15,20]. Altogether, Wnt4 upregulation by verapamil treatment may have potential as a therapeutic target regarding T2D and, therefore, requires further in-depth studies.

Mitochondrial dysfunction is related to pathophysiology of diabetes, resulting in impaired ATP production and defective insulin secretion. VDAC, a key protein found in the outer mitochondrial membrane, regulates the movement of metabolites across the membrane [51], and is a key element in apoptotic signaling [52]. VDAC1 overexpression in various cells has been shown to induce apoptotic cell death [52], and it increased the susceptibility to apoptosis in response to high glucose conditions [53], suggesting its regulatory role as a gatekeeper in mitochondria-mediated apoptosis. *VDAC1* overexpression was found to be driven by impaired glycemic levels and its inhibition restored GSIS and prevented hyperglycemia in *db*/*db* mice [54]. Of note, we found that verapamil treatment downregulated protein expression of both VDAC isoforms (VDAC1/2); and considering that VDAC1 was upregulated by a state of glucotoxicity over a prolonged period in pre-diabetic patients [53–55], verapamil could be an ideal therapy to prevent both the development and progression of diabetes. Taken together, based on growing numbers of studies, we suggest that the anti-diabetic benefit of verapamil could be attributed to: (i) decreased TXNIP mRNA expression [15], (ii) CCK upregulation [47], (iii) Wnt4 upregulation [49], (iv) increased mRNA and protein levels of CaMK4 [56], and/or (v) downregulation of VDAC 1/2 [52].

Although our study provides valuable insights into the molecular and cellular mechanisms that are altered by verapamil, it involves certain limitations. Firstly, we have used a single cell-line (MIN6 cells) and.it would be interesting to also study effects of verapamil on other β cell lines and primary isolated islets. Next, the role of genes such as *Wnt4* must be inferred with caution, owing to their heterogeneity and biphasic involvement in both canonical and non-canonical pathways, and mainly due to a lack of deeper understanding of their precise role in diabetes and related disorders. Further studies are required to elucidate the exact role of such factors.

5. Conclusions

Taken together, our data suggests that the pretreatment with verapamil may render protection in MIN6 β-cells and zebrafish larvae, following exposure to T1D/T2D mimicking conditions. Characteristic changes identified in the β-cell proteomic and transcriptomic landscapes after verapamil treatment provide valuable insights into the critical molecular reprogramming induced by verapamil, enabling the development of novel strategies targeted at treating diabetes at its root cause i.e., by resolving β-cell loss or impairment.

Supplementary Materials: The following supporting information can be downloaded at: www.mdpi.com/xxx/s1, Figure S1: Pancreatic secretion (KEGG: 04972); and Supplementary Methods.

Author Contributions: Conceptualization, Hossein Arefanian, Ashraf Al Madhoun, Fatema Al-Rashed, Fawaz Alzaid, Fatemah Bahman and Fahd Al-Mulla; Funding acquisition, Hossein Arefanian, Ashraf Al Madhoun, Rasheed Ahmad and Fahd Al-Mulla; Investigation, Hossein Arefanian, Ashraf Al Madhoun, Fatema Al-Rashed, Fawaz Alzaid, Fatemah Bahman, Rasheeba Nizam, Sardar Sindhu, Mohamed Abu-Farha, Rasheed Ahmad and Fahd Al-Mulla; Methodology, Hossein Arefanian, Ashraf Al Madhoun, Fatema Al-Rashed, Fawaz Alzaid, Fatemah Bahman, Rasheeba Nizam, Mohammed Alhusayan, Sumi John, Sindhu Jacob, Michayla Williams,

Nermeen Abu Khalaf, Steve Shenouda, Shibu Joseph, Halemah AlSaeed, Shihab Kochumon, Mohamed Abu-Farha and Fahd Al-Mulla; Supervision, Hossein Arefanian, Ashraf Al Madhoun, Fatema Al-Rashed, Fawaz Alzaid, Mohamed Abu-Farha, Jehad Abubaker, Thangavel Alphonse Thanaraj, Rasheed Ahmad and Fahd Al-Mulla; Visualization, Hossein Arefanian, Ashraf Al Madhoun, Fatema Al-Rashed, Rasheeba Nizam, Mohammed Alhusayan, Sumi John, Michayla Williams, Nermeen Abu Khalaf, Steve Shenouda and Sardar Sindhu; Writing – original draft, Hossein Arefanian, Ashraf Al Madhoun, Fatema Al-Rashed, Fatemah Bahman, Rasheeba Nizam, Lubaina Koti, Sardar Sindhu, Mohamed Abu-Farha and Fahd Al-Mulla; Writing – review & editing, Hossein Arefanian, Ashraf Al Madhoun, Fatema Al-Rashed, Fawaz Alzaid, Anwar Mohammad, Lubaina Koti, Sardar Sindhu, Mohamed Abu-Farha, Jehad Abubaker, Thangavel Alphonse Thanaraj, Rasheed Ahmad and Fahd Al-Mulla.

Funding: This work was funded by Kuwait Foundation for the Advancement of Sciences (KFAS) under project number RA CB-2021-007.

Institutional Review Board Statement: The zebrafish study was conducted as per the guidelines approved by the Dasman Diabetes Institute Animal Care Ethical Committee (RA-2019-005) in accordance with the National Institutes of Health guide for the care and use of Laboratory animals (NIH Publications No. 8023, revised 1978) and in compliance with the ARRIVE guidelines as well as the standard laboratory procedures for zebrafish.

Data Availability Statement: All data associated with the article are available on request from the corresponding author.

Acknowledgments: This work was funded by Kuwait Foundation for the Advancement of Sciences (KFAS) under project number RA CB-2021-007.

Conflicts of Interest: The authors declare no conflicts of interest.

References

1. Sun, H.; Saeedi, P.; Karuranga, S.; Pinkepank, M.; Ogurtsova, K.; Duncan, B.B.; Stein, C.; Basit, A.; Chan, J.C.N.; Mbanya, J.C.; et al. IDF Diabetes Atlas: Global, regional and country-level diabetes prevalence estimates for 2021 and projections for 2045. *Diabetes Research and Clinical Practice* **2022**, *183*, 109119. https://doi.org/.
2. von Scholten, B.J.; Kreiner, F.F.; Gough, S.C.L.; von Herrath, M. Current and future therapies for type 1 diabetes. *Diabetologia* **2021**, *64*, 1037-1048. https://doi.org/10.1007/s00125-021-05398-3.
3. Xu, G.; Grimes, T.D.; Grayson, T.B.; Chen, J.; Thielen, L.A.; Tse, H.M.; Li, P.; Kanke, M.; Lin, T.T.; Schepmoes, A.A.; et al. Exploratory study reveals far reaching systemic and cellular effects of verapamil treatment in subjects with type 1 diabetes. *Nature communications* **2022**, *13*, 1159. https://doi.org/10.1038/s41467-022-28826-3.
4. Butler, A.E.; Janson, J.; Bonner-Weir, S.; Ritzel, R.; Rizza, R.A.; Butler, P.C. Beta-cell deficit and increased beta-cell apoptosis in humans with type 2 diabetes. *Diabetes* **2003**, *52*, 102-110. https://doi.org/10.2337/diabetes.52.1.102.
5. Davis, A.K.; DuBose, S.N.; Haller, M.J.; Miller, K.M.; DiMeglio, L.A.; Bethin, K.E.; Goland, R.S.; Greenberg, E.M.; Liljenquist, D.R.; Ahmann, A.J.; et al. Prevalence of detectable C-Peptide according to age at diagnosis and duration of type 1 diabetes. *Diabetes care* **2015**, *38*, 476-481. https://doi.org/10.2337/dc14-1952.
6. Messerli, F.H. "Cardioprotection"--not all calcium antagonists are created equal. *Am J Cardiol* **1990**, *66*, 855-856. https://doi.org/10.1016/0002-9149(90)90364-7.
7. Cooper-Dehoff, R.; Cohen, J.D.; Bakris, G.L.; Messerli, F.H.; Erdine, S.; Hewkin, A.C.; Kupfer, S.; Pepine, C.J. Predictors of development of diabetes mellitus in patients with coronary artery disease taking antihypertensive medications (findings from the INternational VErapamil SR-Trandolapril STudy [INVEST]). *Am J Cardiol* **2006**, *98*, 890-894. https://doi.org/10.1016/j.amjcard.2006.04.030.
8. Cooper-DeHoff, R.M.; Aranda, J.M., Jr.; Gaxiola, E.; Cangiano, J.L.; Garcia-Barreto, D.; Conti, C.R.; Hewkin, A.; Pepine, C.J. Blood pressure control and cardiovascular outcomes in high-risk Hispanic patients--findings from the International Verapamil SR/Trandolapril Study (INVEST). *American heart journal* **2006**, *151*, 1072-1079. https://doi.org/10.1016/j.ahj.2005.05.024.
9. Yin, T.; Kuo, S.-C.; Chang, Y.-Y.; Chen, Y.-T.; Wang, K.-W.K. Verapamil Use Is Associated With Reduction of Newly Diagnosed Diabetes Mellitus. *The Journal of Clinical Endocrinology & Metabolism* **2017**, *102*, 2604-2610. https://doi.org/10.1210/jc.2016-3778.
10. Khodneva, Y.; Shalev, A.; Frank, S.J.; Carson, A.P.; Safford, M.M. Calcium channel blocker use is associated with lower fasting serum glucose among adults with diabetes from the REGARDS study. *Diabetes Res Clin Pract* **2016**, *115*, 115-121. https://doi.org/10.1016/j.diabres.2016.01.021.
11. Ovalle, F.; Grimes, T.; Xu, G.; Patel, A.J.; Grayson, T.B.; Thielen, L.A.; Li, P.; Shalev, A. Verapamil and beta cell function in adults with recent-onset type 1 diabetes. *Nature medicine* **2018**, *24*, 1108-1112. https://doi.org/10.1038/s41591-018-0089-4.

12. Wang, C.Y.; Huang, K.C.; Lu, C.W.; Chu, C.H.; Huang, C.N.; Chen, H.S.; Lee, I.T.; Chen, J.F.; Chen, C.C.; Chen, C.S.; et al. A Randomized Controlled Trial of R-Form Verapamil Added to Ongoing Metformin Therapy in Patients with Type 2 Diabetes. *The Journal of clinical endocrinology and metabolism* **2022**, *107*, e4063-e4071. https://doi.org/10.1210/clinem/dgac436.
13. Forlenza, G.P.; McVean, J.; Beck, R.W.; Bauza, C.; Bailey, R.; Buckingham, B.; DiMeglio, L.A.; Sherr, J.L.; Clements, M.; Neyman, A.; et al. Effect of Verapamil on Pancreatic Beta Cell Function in Newly Diagnosed Pediatric Type 1 Diabetes: A Randomized Clinical Trial. *Jama* **2023**, *329*, 990-999. https://doi.org/10.1001/jama.2023.2064.
14. Malayeri, A.; Zakerkish, M.; Ramesh, F.; Galehdari, H.; Hemmati, A.A.; Angali, K.A. The Effect of Verapamil on TXNIP Gene Expression, GLP1R mRNA, FBS, HbA1c, and Lipid Profile in T2DM Patients Receiving Metformin and Sitagliptin. *Diabetes therapy: Research, treatment and education of diabetes and related disorders* **2021**, *12*, 2701-2713. https://doi.org/10.1007/s13300-021-01145-4.
15. Xu, G.; Chen, J.; Jing, G.; Shalev, A. Preventing β-cell loss and diabetes with calcium channel blockers. *Diabetes* **2012**, *61*, 848-856. https://doi.org/10.2337/db11-0955.
16. Borowiec, A.M.; Właszczuk, A.; Olakowska, E.; Lewin-Kowalik, J. TXNIP inhibition in the treatment of diabetes. Verapamil as a novel therapeutic modality in diabetic patients. *Medicine and pharmacy reports* **2022**, *95*, 243-250. https://doi.org/10.15386/mpr-2187.
17. Chen, J.; Cha-Molstad, H.; Szabo, A.; Shalev, A. Diabetes induces and calcium channel blockers prevent cardiac expression of proapoptotic thioredoxin-interacting protein. *American journal of physiology. Endocrinology and metabolism* **2009**, *296*, E1133-1139. https://doi.org/10.1152/ajpendo.90944.2008.
18. Carnovale, C.; Dassano, A.; Mosini, G.; Mazhar, F.; D'Addio, F.; Pozzi, M.; Radice, S.; Fiorina, P.; Clementi, E. The β-cell effect of verapamil-based treatment in patients with type 2 diabetes: A systematic review. *Acta diabetologica* **2020**, *57*, 117-131. https://doi.org/10.1007/s00592-019-01370-1.
19. Poudel, R.R.; Kafle, N.K. Verapamil in Diabetes. *Indian journal of endocrinology and metabolism* **2017**, *21*, 788-789. https://doi.org/10.4103/ijem.IJEM_190_17.
20. Chen, J.; Hui, S.T.; Couto, F.M.; Mungrue, I.N.; Davis, D.B.; Attie, A.D.; Lusis, A.J.; Davis, R.A.; Shalev, A. Thioredoxin-interacting protein deficiency induces Akt/Bcl-xL signaling and pancreatic beta-cell mass and protects against diabetes. *FASEB journal: Official publication of the Federation of American Societies for Experimental Biology* **2008**, *22*, 3581-3594. https://doi.org/10.1096/fj.08-111690.
21. Miyazaki, J.; Araki, K.; Yamato, E.; Ikegami, H.; Asano, T.; Shibasaki, Y.; Oka, Y.; Yamamura, K. Establishment of a pancreatic beta cell line that retains glucose-inducible insulin secretion: Special reference to expression of glucose transporter isoforms. *Endocrinology* **1990**, *127*, 126-132. https://doi.org/10.1210/endo-127-1-126.
22. Hu, W.; Wang, R.; Sun, B. Meteorin-Like Ameliorates β Cell Function by Inhibiting β Cell Apoptosis of and Promoting β Cell Proliferation via Activating the WNT/β-Catenin Pathway. *Frontiers in pharmacology* **2021**, *12*, 627147. https://doi.org/10.3389/fphar.2021.627147.
23. El-Sharkawey, A. Calculate the Corrected Total Cell Fluorescence (CTCF). **2016**.
24. Al Madhoun, A.; Marafie, S.K.; Haddad, D.; Melhem, M.; Abu-Farha, M.; Ali, H.; Sindhu, S.; Atari, M.; Al-Mulla, F. Comparative Proteomic Analysis Identifies EphA2 as a Specific Cell Surface Marker for Wharton's Jelly-Derived Mesenchymal Stem Cells. *International journal of molecular sciences* **2020**, *21*. https://doi.org/10.3390/ijms21176437.
25. Al Madhoun, A.; Haddad, D.; Al Tarrah, M.; Jacob, S.; Al-Ali, W.; Nizam, R.; Miranda, L.; Al-Rashed, F.; Sindhu, S.; Ahmad, R.; et al. Microarray analysis reveals ONC201 mediated differential mechanisms of CHOP gene regulation in metastatic and nonmetastatic colorectal cancer cells. *Scientific reports* **2021**, *11*, 11893. https://doi.org/10.1038/s41598-021-91092-8.
26. Pozarowski, P.; Darzynkiewicz, Z. Analysis of cell cycle by flow cytometry. *Methods in molecular biology (Clifton, N.J.)* **2004**, *281*, 301-311. https://doi.org/10.1385/1-59259-811-0:301.
27. Damame, H.H.; Rooge, S.B.; Patil, R.S.; Arvindekar, A.U. In vitro model using cytokine cocktail to evaluate apoptosis in Min6 pancreatic beta cells. *Journal of pharmacological and toxicological methods* **2020**, *106*, 106914. https://doi.org/10.1016/j.vascn.2020.106914.
28. Wang, C.; Guan, Y.; Yang, J. Cytokines in the Progression of Pancreatic β-Cell Dysfunction. *International journal of endocrinology* **2010**, *2010*, 515136. https://doi.org/10.1155/2010/515136.
29. Marafie, S.K.; Al-Shawaf, E.M.; Abubaker, J.; Arefanian, H. Palmitic acid-induced lipotoxicity promotes a novel interplay between Akt-mTOR, IRS-1, and FFAR1 signaling in pancreatic β-cells. *Biological research* **2019**, *52*, 44. https://doi.org/10.1186/s40659-019-0253-4.
30. Orliaguet, L.; Ejlalmanesh, T.; Humbert, A.; Ballaire, R.; Diedisheim, M.; Julla, J.B.; Chokr, D.; Cuenco, J.; Michieletto, J.; Charbit, J.; et al. Early macrophage response to obesity encompasses Interferon Regulatory Factor 5 regulated mitochondrial architecture remodelling. *Nature communications* **2022**, *13*, 5089. https://doi.org/10.1038/s41467-022-32813-z.

31. Abu-Farha, M.; Lambert, J.P.; Al-Madhoun, A.S.; Elisma, F.; Skerjanc, I.S.; Figeys, D. The tale of two domains: Proteomics and genomics analysis of SMYD2, a new histone methyltransferase. *Molecular & cellular proteomics: MCP* **2008**, *7*, 560-572. https://doi.org/10.1074/mcp.M700271-MCP200.
32. Rivera, C.G.; Tyler, B.M.; Murali, T.M. Sensitive detection of pathway perturbations in cancers. *BMC bioinformatics* **2012**, *13 Suppl 3*, S9. https://doi.org/10.1186/1471-2105-13-s3-s9.
33. Kimmel, C.B.; Ballard, W.W.; Kimmel, S.R.; Ullmann, B.; Schilling, T.F. Stages of embryonic development of the zebrafish. *Developmental dynamics: An official publication of the American Association of Anatomists* **1995**, *203*, 253-310. https://doi.org/10.1002/aja.1002030302.
34. Pisharath, H.; Rhee, J.M.; Swanson, M.A.; Leach, S.D.; Parsons, M.J. Targeted ablation of beta cells in the embryonic zebrafish pancreas using E. coli nitroreductase. *Mechanisms of development* **2007**, *124*, 218-229. https://doi.org/10.1016/j.mod.2006.11.005.
35. Westerfield, M. *The zebrafish book. A guide for the laboratory use of zebrafish (Danio rerio)*, 4th ed ed.; Univ. of Oregon Press, Eugene.: 2007.
36. Wachlin, G.; Augstein, P.; Schröder, D.; Kuttler, B.; Klöting, I.; Heinke, P.; Schmidt, S. IL-1beta, IFN-gamma and TNF-alpha increase vulnerability of pancreatic beta cells to autoimmune destruction. *J Autoimmun* **2003**, *20*, 303-312. https://doi.org/10.1016/s0896-8411(03)00039-8.
37. Banu, S.; Sur, D. Role of Macrophage in Type 2 Diabetes Mellitus: Macrophage Polarization a New Paradigm for Treatment of Type 2 Diabetes Mellitus. *Endocrine, metabolic & immune disorders drug targets* **2023**, *23*, 2-11. https://doi.org/10.2174/1871530322666220630093359.
38. Draghici, S.; Khatri, P.; Tarca, A.L.; Amin, K.; Done, A.; Voichita, C.; Georgescu, C.; Romero, R. A systems biology approach for pathway level analysis. *Genome research* **2007**, *17*, 1537-1545. https://doi.org/10.1101/gr.6202607.
39. Tarca, A.L.; Draghici, S.; Khatri, P.; Hassan, S.S.; Mittal, P.; Kim, J.S.; Kim, C.J.; Kusanovic, J.P.; Romero, R. A novel signaling pathway impact analysis. *Bioinformatics (Oxford, England)* **2009**, *25*, 75-82. https://doi.org/10.1093/bioinformatics/btn577.
40. Khatri, P.; Voichita, C.; Kattan, K.; Ansari, N.; Khatri, A.; Georgescu, C.; Tarca, A.L.; Draghici, S. Onto-Tools: New additions and improvements in 2006. *Nucleic acids research* **2007**, *35*, W206-211. https://doi.org/10.1093/nar/gkm327.
41. Bo, S.; Gentile, L.; Castiglione, A.; Prandi, V.; Canil, S.; Ghigo, E.; Ciccone, G. C-peptide and the risk for incident complications and mortality in type 2 diabetic patients: A retrospective cohort study after a 14-year follow-up. *European journal of endocrinology* **2012**, *167*, 173-180. https://doi.org/10.1530/eje-12-0085.
42. Kim, B.-Y.; Jung, C.-H.; Mok, J.-O.; Kang, S.-K.; Kim, C.-H. Association between serum C-peptide levels and chronic microvascular complications in Korean type 2 diabetic patients. *Acta diabetologica* **2012**, *49*, 9-15.
43. Kushner, J.A.; Ciemerych, M.A.; Sicinska, E.; Wartschow, L.M.; Teta, M.; Long, S.Y.; Sicinski, P.; White, M.F. Cyclins D2 and D1 are essential for postnatal pancreatic beta-cell growth. *Molecular and cellular biology* **2005**, *25*, 3752-3762. https://doi.org/10.1128/mcb.25.9.3752-3762.2005.
44. Kang, J.H.; Kim, M.J.; Ko, S.H.; Jeong, I.K.; Koh, K.H.; Rhie, D.J.; Yoon, S.H.; Hahn, S.J.; Kim, M.S.; Jo, Y.H. Upregulation of rat Ccnd1 gene by exendin-4 in pancreatic beta cell line INS-1: Interaction of early growth response-1 with cis-regulatory element. *Diabetologia* **2006**, *49*, 969-979. https://doi.org/10.1007/s00125-006-0179-6.
45. Minn, A.H.; Pise-Masison, C.A.; Radonovich, M.; Brady, J.N.; Wang, P.; Kendziorski, C.; Shalev, A. Gene expression profiling in INS-1 cells overexpressing thioredoxin-interacting protein. *Biochemical and biophysical research communications* **2005**, *336*, 770-778. https://doi.org/10.1016/j.bbrc.2005.08.161.
46. Zhou, R.; Tardivel, A.; Thorens, B.; Choi, I.; Tschopp, J. Thioredoxin-interacting protein links oxidative stress to inflammasome activation. *Nature immunology* **2010**, *11*, 136-140. https://doi.org/10.1038/ni.1831.
47. Lavine, J.A.; Kibbe, C.R.; Baan, M.; Sirinvaravong, S.; Umhoefer, H.M.; Engler, K.A.; Meske, L.M.; Sacotte, K.A.; Erhardt, D.P.; Davis, D.B. Cholecystokinin expression in the β-cell leads to increased β-cell area in aged mice and protects from streptozotocin-induced diabetes and apoptosis. *American journal of physiology. Endocrinology and metabolism* **2015**, *309*, E819-828. https://doi.org/10.1152/ajpendo.00159.2015.
48. Katsumoto, K.; Yennek, S.; Chen, C.; Silva, L.F.D.; Traikov, S.; Sever, D.; Azad, A.; Shan, J.; Vainio, S.; Ninov, N.; et al. Wnt4 is heterogeneously activated in maturing β-cells to control calcium signaling, metabolism and function. *Nature communications* **2022**, *13*, 6255. https://doi.org/10.1038/s41467-022-33841-5.
49. Kurita, Y.; Ohki, T.; Soejima, E.; Yuan, X.; Kakino, S.; Wada, N.; Hashinaga, T.; Nakayama, H.; Tani, J.; Tajiri, Y.; et al. A High-Fat/High-Sucrose Diet Induces WNT4 Expression in Mouse Pancreatic β-cells. *The Kurume medical journal* **2019**, *65*, 55-62. https://doi.org/10.2739/kurumemedj.MS652008.
50. Liu, J.; Li, Y.; Zhou, X.; Zhang, X.; Meng, H.; Liu, S.; Zhang, L.; He, J.; He, Q.; Geng, Y. CaMKIV limits metabolic damage through induction of hepatic autophagy by CREB in obese mice. *The Journal of endocrinology* **2020**, *244*, 353-367. https://doi.org/10.1530/joe-19-0251.

 doi:10.20944/preprints202403.1681.v1

51. De Marchi, U.; Fernandez-Martinez, S.; de la Fuente, S.; Wiederkehr, A.; Santo-Domingo, J. Mitochondrial ion channels in pancreatic β-cells: Novel pharmacological targets for the treatment of Type 2 diabetes. *British journal of pharmacology* **2021**, *178*, 2077-2095. https://doi.org/10.1111/bph.15018.
52. Abu-Hamad, S.; Sivan, S.; Shoshan-Barmatz, V. The expression level of the voltage-dependent anion channel controls life and death of the cell. *Proceedings of the National Academy of Sciences of the United States of America* **2006**, *103*, 5787-5792. https://doi.org/10.1073/pnas.0600103103.
53. Ahmed, M.; Muhammed, S.J.; Kessler, B.; Salehi, A. Mitochondrial proteome analysis reveals altered expression of voltage dependent anion channels in pancreatic β-cells exposed to high glucose. *Islets* **2010**, *2*, 283-292. https://doi.org/10.4161/isl.2.5.12639.
54. Zhang, E.; Mohammed Al-Amily, I.; Mohammed, S.; Luan, C.; Asplund, O.; Ahmed, M.; Ye, Y.; Ben-Hail, D.; Soni, A.; Vishnu, N.; et al. Preserving Insulin Secretion in Diabetes by Inhibiting VDAC1 Overexpression and Surface Translocation in β Cells. *Cell metabolism* **2019**, *29*, 64-77.e66. https://doi.org/10.1016/j.cmet.2018.09.008.
55. Maurya, S.R.; Mahalakshmi, R. VDAC-2: Mitochondrial outer membrane regulator masquerading as a channel? *The FEBS journal* **2016**, *283*, 1831-1836. https://doi.org/10.1111/febs.13637.
56. Persaud, S.J.; Liu, B.; Sampaio, H.B.; Jones, P.M.; Muller, D.S. Calcium/calmodulin-dependent kinase IV controls glucose-induced Irs2 expression in mouse beta cells via activation of cAMP response element-binding protein. *Diabetologia* **2011**, *54*, 1109-1120. https://doi.org/10.1007/s00125-011-2050-7.